4

SiC/SiC Composites for 1200°C and Above

J.A. DiCarlo, H-M. Yun, G.N. Morscher, and R.T. Bhatt

NASA Glenn Research Center
21000 Brookpark Road
Cleveland, Ohio 44135
Phone 216-433-5514
James.A.DiCarlo@NASA.gov

ABSTRACT

The successful replacement of metal alloys by ceramic matrix composites (CMC) in high-temperature engine components will require the development of constituent materials and processes that can provide CMC systems with enhanced thermal capability along with the key thermostructural properties required for long-term component service. This chapter presents information concerning processes and properties for five silicon carbide (SiC) fiber-reinforced SiC matrix composite systems recently developed by NASA that can operate under mechanical loading and oxidizing conditions for hundreds of hours at 1204, 1315, and 1427°C, temperatures well above current metal capability. This advanced capability stems in large part from specific NASA-developed processes that significantly improve the creep-rupture and environmental resistance of the SiC fiber as well as the thermal conductivity, creep resistance, and intrinsic thermal stability of the SiC matrices.

1. INTRODUCTION

As structural materials for high-temperature components in advanced engines for power and propulsion, fiber-reinforced ceramic matrix composites (CMC) offer a variety of performance advantages over the best metallic alloys with current structural capability to ~1100°C.

These advantages are primarily based on the CMC being capable of displaying higher temperature capability, lower density (∼30–50% metal density), and sufficient toughness for damage tolerance and prevention of catastrophic failure. These properties should in turn result in many important benefits for advanced engines, such as reduced cooling air requirements, simpler component design, reduced weight of support structure, improved fuel efficiency, reduced emissions, longer service life, and higher thrust. However, the successful application of CMC will depend strongly on designing and processing the CMC microstructural constituents so that they can synergistically provide the total CMC system with the key thermostructural properties required by the components. The objectives of this chapter are first to discuss in a general manner these property requirements for typical hot-section engine components, and then to show how in recent years advanced CMC constituent materials and processes have been developed by NASA for fabricating various silicon carbide (SiC) fiber-reinforced SiC-matrix (SiC/SiC) composite systems with increasing temperature capability from ∼1200°C to over 1400°C.

2. APPLICATIONS

Much initial progress in identifying the proper CMC constituent materials and processes to achieve the performance requirements of hot-section components in advanced gas turbine engines was made under the former NASA Enabling Propulsion Materials (EPM) Program, which had as one of its primary goals the development of an advanced CMC combustor liner for a future high speed civil transport (HSCT) **[1]**. This progress centered on the development of a SiC/SiC CMC system that addresses many of the general performance needs of combustor liners that are required to operate for many hundreds of hours at an upper use temperature of ∼1200°C. In 1999, the NASA EPM Program was terminated due to cancellation of HSCT research. Subsequently the new NASA Ultra Efficient Engine Technologies (UEET) Program was initiated to explore advanced technologies for a variety of low-emission civilian engine systems, including building on NASA EPM success to develop 1315°C SiC/SiC composite systems for potentially hotter components, such as inlet turbine vanes **[2]**. For hot-section components in space-propulsion engines, the NASA Next Generation Launch Technology (NGLT) program is currently developing SiC/SiC systems with even higher temperature capability since here the primary thermal source is the oxidative combustion of hydrogen fuel rather than jet fuel **[3]**.

Because quantitative property requirements for the various components are engine-specific and often engine company sensitive, the general objective at NASA for all these component development programs has been to develop CMC systems that achieve the upper use temperature goals for hundreds of hours while still displaying, to as high a degree as possible, the key thermo-structural properties needed by a typical hot-section component. To accomplish this objective, a variety of factors had to be optimized within the CMC microstructure, including fiber type, fiber architecture, fiber coating (interphases), and matrix constituents. In order to facilitate this process, NASA selected a short list of first-order property goals that a high-temperature CMC system must display for engine applications. These are listed in the first column of Table 1, which also indicates the technical

TABLE 1. Key CMC Property Goals, Controlling Factors, and Demonstration Tests for CMC Capability

Key CMC Property Goals *(Importance for CMC engine component)*	Key Controlling Constituent Factors	CMC Demonstration Test *(Typically conducted on specimens from thin CMC panels)*
High tensile Proportional Limit Stress (PLS) after CMC processing *(allows high CMC design stress and high environmental resistance)*	Matrix Porosity, Fiber Content	Tensile stress-strain behavior in fiber direction of as-fabricated CMC at 20°C and upper use temperature in air
High Ultimate Tensile Strength (UTS) and strain after CMC processing *(allows good CMC toughness and long life after matrix cracking in aggressive environments)*	Fiber Strength, Fiber Content	Tensile stress-strain behavior in fiber direction of as- fabricated CMC at 20°C and upper use temperature in air
High UTS retention after interphase exposure at intermediate temperatures in wet oxygen *(allows CMC toughness retention when exposed, uncracked or cracked, to combustion gases)*	Fiber Coating Composition	Tensile stress-strain behavior after burner rig exposure near 800°C; Rupture behavior of cracked CMC near 800°C in air
High creep resistance at upper use temperature under high tensile stress *(allows long life, dimensional control, low residual CMC stress)*	Matrix Creep, Fiber Creep	Creep behavior in air at upper use temperature under a constant tensile stress ~60% of matrix cracking stress
Long Rupture life (>500 hours) at upper use temperature under high tensile stress *(allows long-term CMC component service)*	Matrix Rupture, Fiber-Rupture	Rupture life in air at upper use temperature under constant tensile stress ~60% of matrix cracking stress
High thermal conductivity at all service temperatures *(reduces thermal stresses due to thermal gradients and thermal shock)*	Fiber-Coating-Matrix Conductivity, Matrix Porosity	Thermal conductivity from 20°C to upper use temperature

importance of each property goal for a general hot-section CMC component. These goals were specifically selected to address key performance issues for structural CMC in general and for SiC/SiC composites in particular.

Thus for example, it is important that the CMC system display as high a proportional limit stress as possible at all potential service temperatures. This is important for design based on elastic mechanical behavior and for component life since the PLS is closely related to the matrix cracking strength. Therefore, high PLS values will allow the component to carry high combinations of mechanical, thermal, and aerodynamic tensile stresses without cracking. However, unexpectedly higher stress combinations may arise during component service that can locally crack the matrix, thereby causing immediate CMC failure if the fibers are not strong enough or sufficient in volume content to sustain the total stress on the CMC.

In addition, after matrix cracking, CMC failure could occur in undesirably short periods of time if the interphase coating and the fibers were allowed to be degraded by the component service environment as it enters into the CMC through the matrix cracks. For the SiC/SiC components, this attack can be especially serious at intermediate temperatures (~800°C) where oxygen in the engine combustion gases can reach the fibers before being sealed off by slow-growing silica on the matrix crack surfaces. Oxygen primarily attacks the SiC fibers by forming a performance-degrading silica layer on the fiber surfaces, causing fiber-fiber and fiber-matrix bonding. Even a small amount of bonding can eliminate the ability of each fiber to act independently. The detrimental consequence is that if one fiber should fracture, it will cause immediate fracture of other fibers to which it is bonded, thereby causing CMC fracture or rupture at undesirably low stresses and short times.

Also shown in Table 1 are (1) those key constituent factors that CMC theory and practice indicate are the primary elements controlling the various property goals, and (2) the laboratory tests typically employed at NASA to demonstrate CMC system capability for meeting each property goal. For convenience and generality, these tests were usually conducted on specimens machined from thin flat panels fabricated at commercial vendors with the selected CMC constituent materials and processes. NASA's primary objective was not to perform exhaustive testing, but only to use the test results to show directions for advanced CMC systems. As a result, the property databases presented here for the various CMC systems are necessarily limited. It is assumed that by examining the first-level property data, engine designers will be able to select the CMC systems that best meet their component performance requirements, and then initiate with a commercial vendor more extensive efforts for CMC system and component evaluation.

Although not discussed here, NASA has also shown that oxide-based environmental barrier coatings (EBC) need to be applied to the hot surfaces of Si-based (SiC, Si_3N_4, SiC/SiC) components in order to realize long-term service in high temperature combustion environments **[4]**. Under these wet oxidizing conditions, growing silica on the CMC surface reacts with water to form volatile species, giving rise to paralinear oxidation kinetics and a gas velocity-dependent recession of the Si-based materials [**5**]. For example, for a lean-burn situation with combustion gases at 10 atm and 90 m/sec velocity, SiC materials are predicted to recess ~250 and 500 μm after 1000 hrs at material temperatures of 2200°F (1204°C) and 2400°F (1315°C), respectively.

3. PROCESSING

Table 2 lists some key constituent material and process data for five SiC fiber-reinforced CMC systems recently developed at NASA. For convenience, these systems have been labeled by the prefix N for NASA, followed by their approximate upper temperature capability in degrees Fahrenheit divided by 100; that is, N22, N24, and N26, with suffix letters A, B, and C to indicate their generation. Also shown in Table 2 are the primary organizations where the different process steps were performed to fabricate each CMC system into a test panel. However, it should be noted that these steps have also been performed at other organizations, resulting in test panels with equivalent properties.

The baseline processing route selected for fabricating the five CMC systems and demonstrating their performance against the Table 1 property goals is shown schematically in

TABLE 2. Key Constituent Material and Process Data for NASA-developed CMC Systems

CMC System	N22	N24-A	N24-B	N24-C	N26-A
Upper Use Temperature	2200°F (1204°C)	2400°F (1315°C)	2400°F (1315°C))	2400°F (1315°C)	2600°F (1427°C)
Fiber Type	Sylramic *(Dow Corning)*	Sylramic-iBN *(Dow Corning + N)*	→	→	→
Interphase Coating	CVI Si-doped BN *(GEPSC)*	→	CVI Si-doped BN outside debond *(GEPSC + N)*	→	→
Matrix	CVI SiC – low content *(GEPSC)*	→	→	CVI SiC – medium content *(GEPSC + N)*	CVI SiC – medium content *(GEPSC)*
	SiC slurry infiltration *(GEPSC)*	→	→		PIP SiC (Polymer Infiltrate and Pyrolysis *(Starfire + N)*
	Silicon melt infiltration *(GEPSC)*	→	→	Silicon melt infiltration *(N)*	

* N = NASA processing.

Fig. 1. As indicated, it involves (1) selecting a high-strength small-diameter SiC fiber type that is commercially available as multi-fiber tows on spools, (2) textile-forming the tows into architectural preforms required by the CMC component or CMC test panel, (3) using conventional chemical vapor infiltration (CVI) methods to deposit thin crack-deflecting interfacial coatings on the fiber surfaces, and (4) over-coating the interfacial coatings with a CVI SiC matrix to a controlled thickness, weight gain, or volume content.

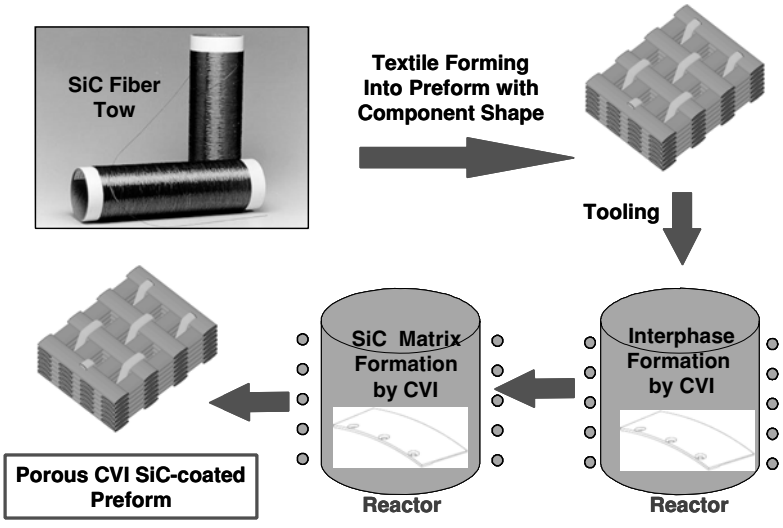

FIGURE 1. Baseline processing route for the NASA CMC systems.

Besides providing environment protection to the interfacial coating, the CVI SiC matrix functions as a strong, creep-resistant, and thermally conductive CMC constituent. However its deposition is not taken to completion because this would trap pores between tows in the fiber architecture, thereby not allowing maximum matrix contribution to the thermal conductivity of the composite system. Depending on the intended CMC upper use temperature, the remaining open porosity in the CVI SiC matrix is then filled with ceramic-based and/or metallic-based materials. Although the filler material in the "hybrid" SiC matrix could serve a variety of functions, its composition and content are typically selected in order to achieve as high a CMC thermal conductivity and as low a CMC porosity as possible.

In general, the baseline processing route of Fig. 1 provides a significant amount of flexibility, particularly in regard to the four key steps involving selection of (1) SiC fiber type, (2) interfacial coating composition, (3) remaining open porosity in the CVI SiC matrix, and (4) infiltration approach(es) to fill this porosity and form the hybrid matrix. As will be discussed in the following, this flexibility was indeed needed in order to optimize the microstructure of the CMC systems in terms of temperature capability and thermostructural properties. Another advantage of this processing route is that it could be used with any textile-formed 2D or 3D architectural preform, which is especially advantageous for fabricating complex-shaped CMC components. In addition, this route can be practiced by any of the many current CMC fabricators who have the capability for interphase and SiC matrix formation by CVI.

3.1. N22 CMC System

During development of the N22 CMC system ($\sim$1997), the only commercially available small-diameter ceramic fiber types with sufficient high-temperature capability were the Sylramic SiC fiber from Dow Corning and the carbon-rich Hi-Nicalon SiC fiber from Nippon Carbon. However, in comparison to the Sylramic fiber, the non-stoichiometry, low process temperature, and carbon-rich surface of the Hi-Nicalon fiber resulted in reduced thermal conductivity, thermal stability, creep resistance, and environmental durability, both for individual fibers **[6]** and their composites. Thus the selected fiber type for the N22 system was the Sylramic SiC fiber, which is no longer produced by Dow Corning, but by ATK COI Ceramics. This fiber type is fabricated by the polymer route in which precursor fibers based on polycarbosilane are spun into multi-fiber tows and then cured, pyrolyzed, and sintered at high temperature ($>1700^{\circ}$C) using boron-containing sintering aids. The sintering process results in very strong fibers (>3 GPa) that are dense, oxygen-free, near stoichiometric, and contain $\sim$1 and $\sim$3 weight % of boron and TiB_2, respectively. To provide enhanced handling and weaving capability, the Sylramic tows were coated by Dow Corning with a polymer-derived Sizing A, which tended to separate contacting fibers in textile-formed preforms. This fiber spreading process typically resulted in better CMC thermostructural properties, such as elastic modulus, ultimate tensile strength (UTS), and rupture strength at intermediate and high temperatures.

For the interfacial coating composition, CVI-produced silicon-doped BN as deposited by GE Power Systems Composites (GEPSC) (formally Honeywell Advanced Composites) was selected because BN not only displays sufficient compliance for matrix crack

deflection around the fibers, but also because it is more oxidatively resistant than traditional carbon-based coatings. When doped with silicon, the BN showed little loss in compliance, but an improvement in its resistance to moisture, which is an advantage during removal of the preforms from the CVI BN reactor into ambient air and their subsequent transportation to the CVI SiC matrix reactor.

For the N22 CMC system, remaining open porosity in the CVI SiC matrix was filled by room-temperature infiltration of SiC particulate or slurry casting, followed by the melt-infiltration (MI) of silicon metal near 1400°C. This yielded a final composite with ∼2% closed porosity within the fiber tows and ∼0% porosity between the tows. The final composite system (often referred to as a slurry-cast MI composite) typically displayed a thermal conductivity about double that of a full CVI SiC composite system in which the CVI matrix process was carried to completion. Also the composite did not require an oxidation-protective over-coating to seal open porosity. Decreasing the porosity of the hybrid matrix also increased the N22 CMC elastic modulus, which in turn contributed to a high proportional limit stress. However, since the filler contained some low-modulus silicon, the modulus increase was not as great as if the filler were completely dense SiC.

3.2. N24-A CMC System

When the property data for the N22 CMC system were analyzed using composite theory and microstructural analysis, certain issues were identified with the fiber, interphase coating, and matrix that indicated that more modifications of these constituents were needed in order to achieve CMC systems for 2400°F (1315°C) components. For example, despite displaying enhanced properties in comparison to other ceramic fiber types, issues related to certain factors existing in the bulk and on the surface of the as-produced Sylramic fiber were found to limit its thermostructural performance, both as individual fibers **[6]** and as textile-formed architectural preforms for SiC/SiC composites. Most importantly, excess boron in the fiber bulk was typically located on the fiber grain boundaries, thereby inhibiting the fiber from displaying the optimum in creep resistance, rupture resistance, and thermal conductivity associated with its grain size. Also in the presence of oxygen-containing environments during composite fabrication or service, boron on the fiber surface had the potential of promoting detrimental silica-based (SiO_2) glass formation that would bond neighboring fibers together and yield as-produced composites with degraded ultimate tensile strength. This mechanical interaction issue was further compounded by a high surface roughness of the Sylramic fiber, which was related to its grain size and ultimately to its high production temperature **[6]**. In addition, although Sizing A helped in reducing the roughness issue, during preform warm-up to the temperatures for deposition of the BN interfacial coating, it decomposed and left a continuous carbon-rich char on the fiber surface, which was then trapped under the BN coating. It was found that this continuous carbon layer extended to the composite surface along the 90° tows; so that upon exposure to flowing combustion gas, oxygen was able to enter the CMC microstructure, volatilize the carbon layer throughout the system, and silica-bond the fibers together **[7]**.

For the N24-A system, these issues surrounding the as-produced Sylramic fiber and its sizing were first overcome by using Sylramic fibers with an alternate Sizing B that yielded much less carbon char than Sizing A. In addition, NASA developed a thermal treatment in

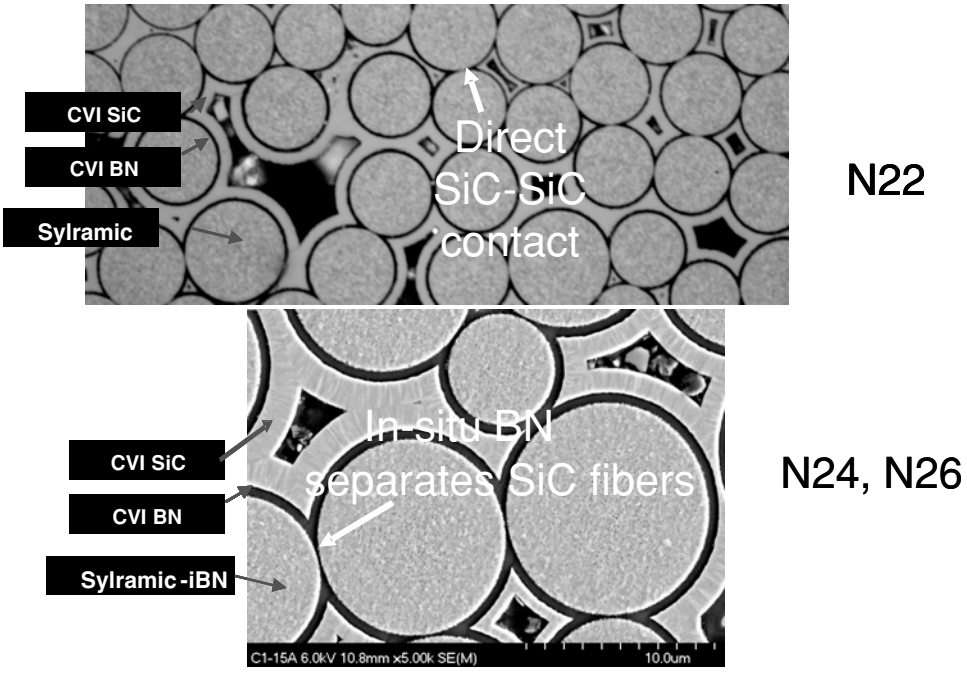

FIGURE 2. SEM micrographs showing that in contrast to the Sylramic N22 CMC system, the in-situ grown BN layer on the Sylramic-iBN fiber is advantageous for physically separating oxidation-prone SiC fiber surfaces within multi-fiber tows in the N24 and N26 systems.

a controlled nitrogen environment that allowed mobile boron sintering aids in the Sylramic fiber to diffuse out of the fiber and to form a thin in-situ grown BN layer on each fiber surface [**8**]. Removing boron from the fiber bulk significantly improved fiber creep, rupture, and oxidation resistance, while the in-situ BN provided a buffer layer that inhibited detrimental chemical attack from inadvertent oxygen and also reduced detrimental mechanical interactions between contacting fibers. The Scanning Electron Microscopy (SEM) photos in Fig. 2 show that this latter mechanism is indeed a key concern for the as-produced Sylramic fibers in the N22 CMC system, since textile forming of tows typically forces direct contact between neigboring fibers (dark rings are CVI BN interphase coatings). However, as also shown in Fig. 2, this issue is less likely with the Sylramic-iBN fibers in the N24-A system, where direct contact between SiC fiber surfaces cannot be observed due to the thin (∼150 nm) in-situ BN layer that completely surrounds each fiber (dark rings contain both CVI BN and in-situ BN coatings). As will be shown in the Properties section, this in-situ BN layer allows the N24-A CMC system to display enhanced behavior, not only for upper use temperature capability, but also for all key fiber-controlled CMC properties. Thus besides providing SiC fibers with improved performance, another advantage of the NASA fiber thermal treatment was the formation of an in-situ grown BN-based fiber coating, which in effect allows the improved fiber properties to be better retained in textile-formed fiber architectures and CMC structures.

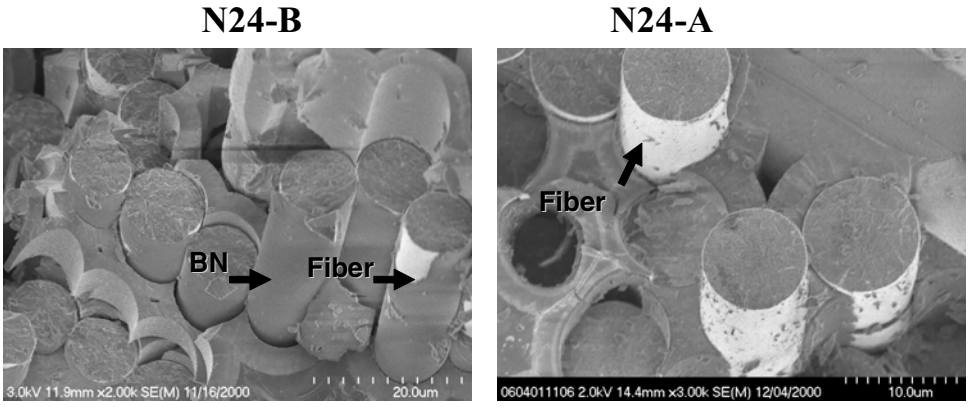

FIGURE 3. SEM micrographs showing (a) outside debonding for the N24-B CMC system and (b) inside debonding for the N24-A system. Note that the BN adheres to the Sylramic-iBN fibers in the outside debonding composites.

3.3. N24-B CMC System

With development of the high performance Sylramic-iBN SiC fiber, the N24-A system showed improvements in practically all the Table 1 properties. Of particular importance in terms of enhanced CMC reliability was an improvement in environmental durability at intermediate temperatures by elimination of the carbon char from Sizing A and by the insertion of an in-situ grown BN surface layer between contacting SiC fibers. As suggested by Fig. 2b, the in-situ grown BN layer delayed SiC-SiC fiber bonding by simply providing an oxidation resistant physical barrier between fibers whenever the fiber tows were exposed to oxygen either during CMC fabrication or during matrix cracking.

Another NASA-developed approach that further improves CMC durability is the basis for the next generation 2400°F CMC system, N24-B. This approach, which is often referred to as "outside debonding", allows the Si-doped BN interphase coating to remain on the fibers during matrix cracking, thereby providing additional environmental protection to the fibers **[9]**. It is accomplished in a proprietary manner by creating simple constituent and process conditions during composite fabrication that assure that the CVI BN interphase coating is already "outside debonded" from the CVI SiC matrix in the as-fabricated CMC. Even though the interphase coating is attached to the fiber and debonded from the matrix, load transfer between the fibers and matrix is still maintained due to the complex-shaped fiber architectures that allowed the interphases to mechanically slide against the matrix during the application of stress. Figs. 3a and 3b compare, respectively, typical fracture surfaces of the N24-A CMC with an "inside debonding" BN interphase coating and the N24-B with an "outside debonding" BN interphase. In comparison to multi-layer concepts for interphase coatings, this outside debonding approach avoids the fabrication of complex interphase compositions and structures, does not rely on uncertain microstructural conditions for matrix crack deflection outside of the interphase, and provides a more reliable approach for retention of the total interphase on the fiber surface. In addition, this approach also reduces CMC elastic modulus and increases CMC ultimate fracture strain, which can be

beneficial, respectively, for reducing thermal stresses within the CMC and increasing its damage tolerance. Thus the N24-B CMC system is more environmentally durable, more damage tolerant, and potentially more resistant to thermal gradients than the N24-A system. However, as a result of "outside debonding, the N24-B system displays a slightly lower thermal conductivity than N24-A.

3.4. N24-C CMC System

Besides improving the fiber and interphase coating for the N24 system, NASA also sought to minimize property limitations associated with the as-produced CVI SiC matrix. These matrix limitations relate to the fact that for best infiltration into the textile-formed fiber tows, the CVI SiC matrix deposition process is typically conducted at temperatures below 1100°C, which is below the application temperatures where the CMC systems will have their greatest practical benefits. Under these processing conditions, although the SiC matrix is fairly dense, its microstructure contains meta-stable atomic defects and is non-stoichiometric due to a small amount of excess silicon. These defects can exist at the matrix grain boundaries where they act as scatterers for thermal phonons and enhance matrix creep by grain-boundary sliding, thereby allowing the matrix and CMC to display less than optimal thermal conductivity and creep-resistance. NASA determined that by using thermal treatments above 1600°C on the CVI SiC-coated preforms prior to the N24 process steps of slurry casting and melt infiltration, excess silicon and process-related defects in the CVI SiC matrix could be removed, yielding the N24-C CMC system with significantly improved creep resistance and thermal conductivity **[10]**. To maximize these benefits as well as the CMC life, the CVI SiC content of the N24-C preform is increased over that typically used in the N24-A and N24-B systems, but only to the point of avoiding significant trapped porosity. The N24-C preform is then thermally treated in argon, and remaining porosity is filled by the melt infiltration of silicon. As indicated in Table 2, the increase in CVI SiC content for the N24-C CMC system also allows elimination of the slurry infiltration step and its associated production costs.

As shown in Fig. 4, the Sylramic-iBN fiber is the only high-strength SiC fiber type that allows preforms with low CVI SiC content (∼20 vol.%) to survive thermal exposure in argon above 1600°C with no loss in ultimate tensile strength of the preform. For the other fiber types in Fig. 4, part of their strength loss could be intrinsic caused by non-optimized microstructures or lower production temperatures **[6]**, and part could be extrinsic caused by fiber attack from inadvertent excess oxygen in the CVI BN fiber coating or from the excess silicon that diffuses out of the CVI SiC matrix during thermal treatment. Since it is well known that BN produced at high temperatures is resistant to oxygen and molten silicon, the better performance of the Sylramic-iBN fiber in Fig. 4 might be expected given its higher production temperature and its in-situ grown BN layer. However, at the higher CVI SiC content used for the N24-C CMC system, thermal exposure resulted in a CMC strength loss of up to 30%. This effect was presumably due to an increase in excess silicon with increasing CVI SiC content, and thus more likelihood of silicon attack of the Sylramic-iBN fiber through the in-situ grown BN layer. In addition, during the high-temperature preform treatment, the BN interphase coating, which was deposited below 1000°C (1830°F), densified and contracted between the fiber and matrix. This in turn caused an automatic "outside debonding" of the BN interphase coating from the matrix, as evidenced by a

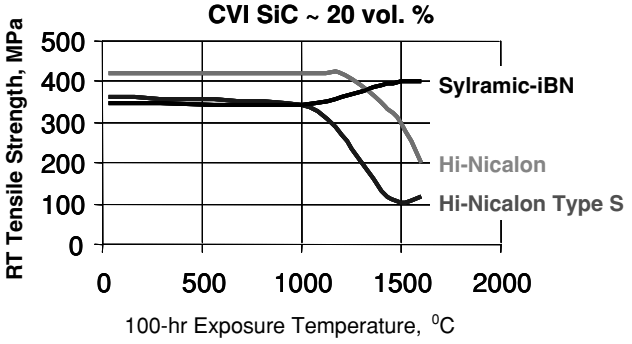

FIGURE 4. Average ultimate tensile strength (UTS) retained at room temperature for various 2D preform panels fabricated by the baseline processing route of Fig. 1 and subjected to 100-hr exposures at high temperatures in argon.

reduced CMC modulus of the final CMC. Thus the N24-C CMC system is more creep resistant, more intrinsically stable, and more thermally conductive than the N24-B system, but at the expense of a lower ultimate strength.

3.5. N26-A CMC System

As described above, small quantities of excess silicon (<1 vol.%) in the as-produced CVI SiC matrix are able to cause a limited attack of the SiC fibers during the high-temperature processing of the N24-C system. The degrading effect of excess silicon from the melt infiltration step was also observed for the N24 CMC systems when they were evaluated for long-term use at potential service temperatures of 2600°F (1427°C) and higher. However in this case, the attack was much more serious and caused primarily by the much greater silicon content (~15 vol.%) introduced by the MI step. The SEM micrograph of Fig. 5 shows an example of this attack for a N24-A CMC system that was thermally exposed at 2552°F (1400°C) in argon for 100 hours under zero stress **[11]**. It can be seen that silicon from the melt-infiltration step was able to diffuse through the grain boundaries of the CVI SiC matrix, attack the BN coatings and SiC fibers, and severely degrade composite strength. The higher CVI SiC content of the N24-C CMC system helps to slow down this attack **[11]**, but not enough to use this system for over 1000 hours at 2400°F or over 100 hours at 2600°F **[12]**.

To address the temperature issues related to excess silicon, all the same constituents in the N24-C system are used for potential N26 CMC generations, but remaining open pores in the CVI SiC matrix are filled by silicon-free ceramics, rather than by melt infiltration of silicon. In particular, for the N26-A CMC system, a SiC-yielding polymer from Starfire Inc. **[13]** is infiltrated into the matrix porosity at room temperature and then pyrolyzed at temperatures up to 2912°F (1600°C). This polymer infiltration and pyrolysis (PIP) process was repeated a few times until composite porosity was reduced to ~14 vol.%. At this point, the total CMC system is then thermally treated at NASA to improve its thermal conductivity and creep-resistance. Thus although more porous than the other CMC systems, the N26-A system has no free silicon in the matrix, thereby allowing long-time structural use at 2600°F

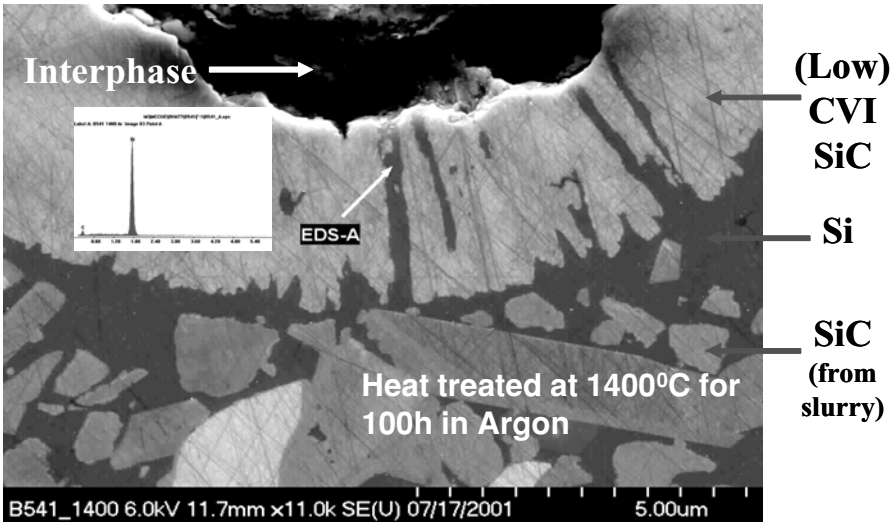

FIGURE 5. SEM micrograph showing degradation of the SiC fiber and BN interphase coating after 100-hr thermal exposure of the N24-A CMC system in argon under zero stress at 2552°F (1400°C). Degradation is due to diffusion through the CVI SiC matrix of the silicon from the melt-infiltration step of the N22 and N24 CMC systems.

(1427°C) and higher. Research is on-going at NASA to develop further generations of the N26-A system where porosity is significantly reduced, so that CMC thermal conductivity can be enhanced beyond the matrix annealing step.

4. PROPERTIES

Based on the property goals of Table 1 and the constituent-process data of Table 2, this section presents key physical and mechanical property data for the five high-temperature CMC systems described above. Composite materials for obtaining these data were fabricated as follows. Sylramic SiC fiber tows were woven into 2D orthogonal fabric with equal tow ends per cm in the 0° (warp) and 90° (fill) directions. The fabric was cut into eight 150 × 230 mm pieces or plies, which were then stacked in a balanced manner to form a thin rectangular-shaped architectural preform. For the N22 system, the stacked plies were then provided directly to GEPSC for BN interphase and partial CVI SiC matrix processing as described in Fig. 1. For the N24 and N26 systems, the stacked plies were converted to Sylramic-iBN fibers at NASA prior to sending to GEPSC. After final matrix processing as described above for the five systems, the stacked fabric preforms were converted into flat CMC test panels with approximate dimensions of 2 × 150 × 230 mm and with total fiber content between 32 and 40 vol.%. It should be noted that a variety of potential CMC engine components, such as combustor liners and shrouds [**1, 14**], are also being made by the laminate or fabric stacking approach, so that the panel property data presented here can be directly used to understand the performance of these components.

For standard measurements of stress-strain and creep-rupture behavior (ASTM C 1337-96), 150 mm long dog-boned shaped tensile specimens with gauge sections of ∼10 mm

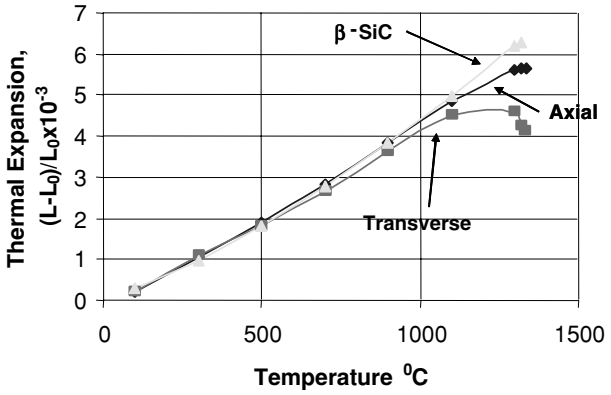

FIGURE 6. Typical linear thermal expansion curves in the axial and transverse directions for the N22 and N24 CMC systems panels fabricated with the silicon melt-infiltration step. Also shown for comparison is the best fit curve for monolithic SiC with the β-phase [16].

width × 25 mm length were machined from each CMC system panel. Each tensile specimen had half of the total fiber fraction aligned along the 150 mm test direction. Composite thermal conductivity was calculated from specimen density data and temperature-dependent data for specimen thermal diffusivity and specific heat. Thermal diffusivity was measured by the thermal flash method in the transverse or through-thickness direction of the test panels. On an absolute basis, the transverse conductivity for a given CMC system was always less than its axial or in-plane conductivity due to the low-conductivity BN interphase.

Table 3 lists some of the important physical properties of the five NASA-developed CMC systems as determined from the as-fabricated test panels. The system densities could be modeled by a simple rule-of-mixtures based on constituent volume fractions and densities [**15**]. All the panels contained an average of ∼36 vol.% fiber and ∼8 vol.% Si-doped BN, which is thick enough for tough composite behavior, but thin enough for CVI SiC matrix penetration into the fiber tows. As the temperature capability requirement increased, the CVI SiC matrix content increased from ∼23 vol.% to ∼35 vol.% to take advantage of the silicon-protective nature, creep-resistance, and thermal conductivity of the CVI SiC composition. For the first four systems, the MI silicon content remained at ∼15 vol.% to derive the benefits of its thermal conductivity and pore-filling capability, but was removed completely from the N26-A system to allow the long lives needed at the higher upper use temperature. Since all the systems contained up to ∼70 vol.% of high-density β-phase SiC grains in the fiber and matrix, their linear thermal expansion behavior was found to be essentially equivalent to that of dense monolithic β-phase SiC. Fig. 6 compares the axial and transverse expansion for the N22 and N24 panels against that of β-phase SiC, which can be described fairly accurately by the following relationship [**16**]:

$$\lambda\,(\%) = \mathrm{T}\,[2.62\ \times 10^{-4}] + \mathrm{T}^2\,[2.314\ \times 10^{-7}] - \mathrm{T}^3\,[0.518\ \times 10^{-10}] \qquad (1)$$

where λ is linear thermal expansion strain and T is in degrees Celsius. The CMC showed a slight deviation from β-phase SiC above 1300°C, which is a characteristic of SiC materials that contain a small amount of free silicon **[17]**. It should be noted that Eq. 1 is not only

TABLE 3. Typical Physical Properties for NASA-developed CMC Systems as 2D Test Panels

Property \ CMC System	N22	N24-A	N24-B	N24-C	N26-A
Upper Use Temperature	2200°F (1204°C)	2400°F (1315°C)	2400°F (1315°C)	2400°F (1315°C)	2600°F (1427°C)
Density, gm/cc	2.85	2.85	2.85	2.76	2.52
Constituent Content, ~Vol.%					
SiC Fiber (3.05 gm/cc)	36	36	36	36	36
Si-BN Interphase (1.5 gm/cc)	8	8	8	8	8
CVI SiC (3.2 gm/cc)	23	23	23	35	35
SiC particulate (3.2 gm/cc)	18	18	18	0	6
Silicon (2.35 gm/cc)	13	13	13	18	0
Porosity	2	2	2	2	14
Thermal Linear Expansion, %	$T\,[2.62 \times 10^{-4}] + T^2\,[2.314 \times 10^{-7}] - T^3\,[0.518 \times 10^{-10}]$ (T = °C)				
Transverse Thermal Conductivity, W/m.C					
204°C (400°F)	24	30	27	41	26
1204°C (2200°F)	15	14	10	17	10

useful for determining CMC linear expansion strain, but also for deriving CMC coefficients of thermal expansion (CTE) at various temperatures.

Typical transverse thermal conductivity data for the CMC panels are listed in Table 3 at 204 and 1204°C, and displayed as a function of temperature in Fig. 7. As with monolithic SiC materials [**18**], the conductivity values increase up to ~200°C and then decrease monotonically with temperature with an approximate inverse temperature dependence. Although both are technically important, transverse rather than in-plane conductivity is generally the first-level property of concern for design of CMC components. This is the case because the components will typically be cooled through their thin wall sections and because the transverse conductivity is typically lower in value, and thus a conservative estimate of material capability. It is affected strongly by matrix composition and porosity, which not only includes the small open and closed pores formed during the matrix infiltration processing steps, but also the long linear pores which are effectively created by poorly conductive interphase coatings on the SiC fibers. The interphase conductivity is dependent both on its composition and its effective contact with the fiber and matrix. Thus wide variation in CMC conductivity is to be expected and has been observed, but qualitative trends are observable. For example, Fig. 7 shows that by changing from the Hi-Nicalon Type S fiber to the Sylramic fiber (N22 system) to the Sylramic-iBN fiber (N24-A system), the transverse conductivities of the Si-containing CMC systems were measurably increased. This reflects on the intrinsic conductivity values for the various fiber types [**6**], and on the ability of the Si-doped BN interphase coating to provide some degree of thermal transport into the fibers. However, as indicated in Table 3, for the N24-B CMC system with an "outside debonding" interphase, a penalty is paid in thermal conductivity due to reduced interphase-matrix contact. This loss was more than recovered when the CVI SiC matrix of the Si-containing N24-C system was annealed. However, another conductivity penalty was taken for the N26-A system when silicon was eliminated and replaced by a hybrid SiC matrix with high porosity.

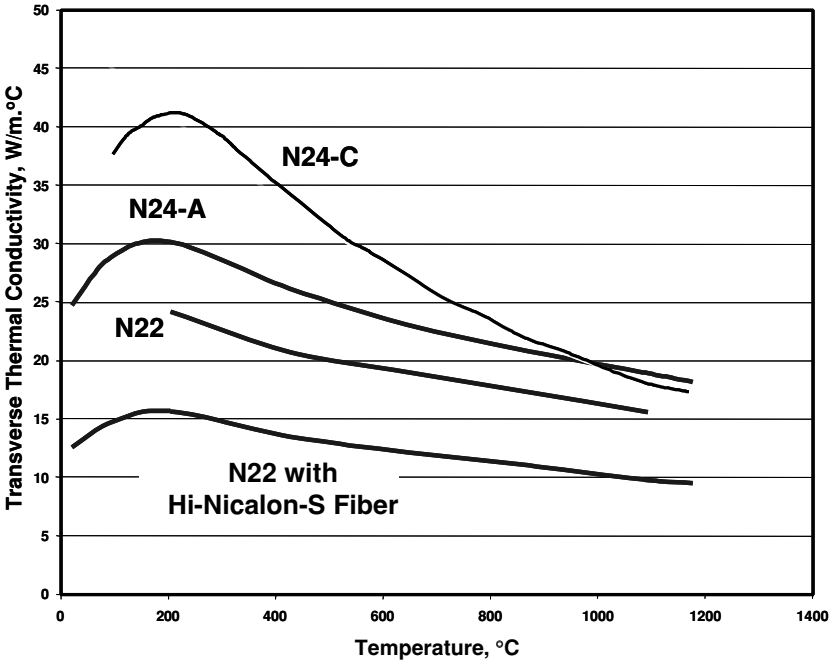

FIGURE 7. Typical transverse thermal conductivity curves for thin panels with CMC systems N22, N24-A, and N24-C. Effect of fiber conductivity is shown by curve for the N22 system with the lower conductivity Hi-Nicalon Type-S fiber type.

Regarding CMC mechanical properties, typical in-plane tensile stress-strain curves at room temperature are shown in Figs. 8 and 9 for the various CMC panels in their as-fabricated condition. Fig. 8 compares the first three systems with inside debonding (N22, N24-A) and with outside debonding (N24-B); whereas Fig. 9 compares the last two systems with annealed matrices and a higher degree of outside debonding (N24-C, N26-A). Using similar curves for multiple test specimens both at room temperature and at their upper use temperature (UUT), Table 4 lists average data for such key mechanical properties as initial elastic modulus, proportional limit stress, ultimate tensile strength, and ultimate tensile strain. It should be noted that since the panels had a range of total fiber content from 32 to 40 vol.%, the data in Table 4 and in the figures, unless otherwise noted, represent average results measured or estimated for a fiber content of ∼36 vol.% total fiber content (∼18 vol.% in the tensile test direction). It should also be noted that elastic moduli of the various systems are reduced at their UUT, but are not presented in Table 4 because due to CMC creep they are dependent on testing stress-rate.

As predicted by CMC theory, some of the Table 4 properties will change significantly with fiber content and test direction. Nevertheless, for the selected fiber content and panel test conditions, qualitative trends can be observed in the as-fabricated CMC mechanical properties at room temperature. For example, regarding elastic modulus, variations between CMC systems can be correlated to the content of the high modulus CVI SiC matrix and to the existence of matrix porosity and/or an outside debonding interphase, both of which

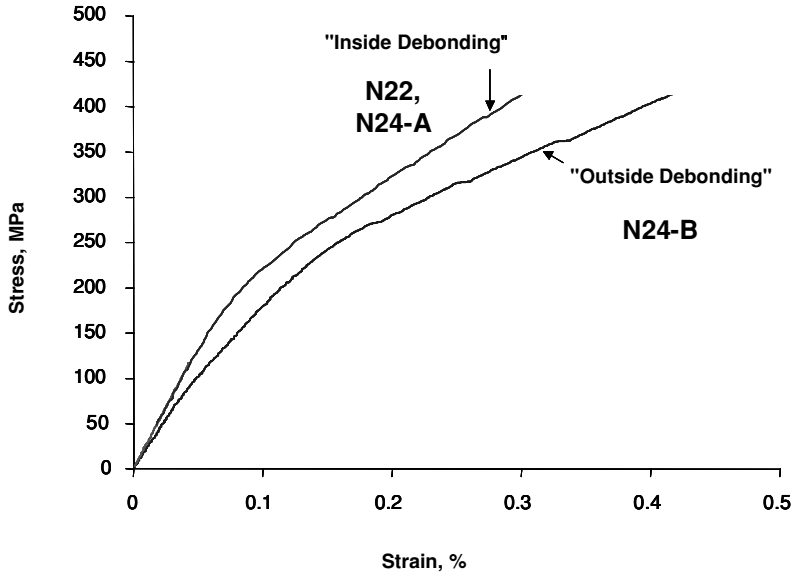

FIGURE 8. Typical room-temperature tensile stress-strain curves for the inside-debonding N22 and N24-A CMC systems, and the outside-debonding N24-B CMC system (total fiber content ∼40 vol.%).

will decrease matrix modulus. The role of outside debonding in reducing matrix modulus is related to the fact that the 90° tows are load-bearing elements within the matrix for CMC loads applied in the 0° test direction. Therefore, when contact between the interphase and matrix is reduced by debonding, loads on 90° tows are reduced, effectively introducing new porosity into the matrix. Regarding CMC proportional limit stress, although the underlying mechanisms are quite complex **[19]**, a very crude rule-of-thumb for 2D 0/90 panels is that the first deviation from stress-strain linearity occurs at approximately ∼0.07%, so that CMC PLS values are approximately proportional to CMC moduli. Regarding CMC ultimate strength, which can be considered to be directly controlled by the in-situ fiber strength, all the Sylramic-iBN fiber systems that were not annealed displayed the highest value of ∼450 MPa.

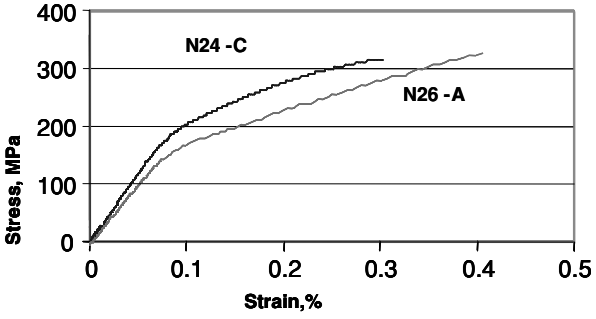

FIGURE 9. Typical room-temperature tensile stress-strain curves for the annealed Sylramic-iBN CMC systems N24-C and N26-A (total fiber content ∼34 vol.%).

TABLE 4. Average Mechanical Properties for NASA-developed CMC Systems (2D 0/90 Test Panels with ~36 vol.% Total Fiber Content

Property* \ CMC System	N22	N24-A	N24-B	N24-C	N26-A
Upper Use Temperature	2200°F (1204°C)		2400°F (1315°C))		2600°F (1427°C)
AS-FABRICATED AT 20°C					
Initial Elastic Modulus, GPa	250	250	210	220	200
Proportional Limit Stress, MPa	180	180	170	160	130
Ultimate Tensile Strength, MPa	400	450	450	310	330
Ultimate Tensile Strain	~0.35%	~0.50%	~0.55%	~0.30%	~0.40%
Interfacial Shear Strength, MPa	~70	~70	~7	<7	<7
AT 800°C					
Ultimate Tensile Strength Retention after 100-hr burner rig	60%	100%	100%		
Rupture Strength, 100 hr, air, MPa	200	200	240		
AT OR NEAR UPPER USE TEMPERATURE					
(Test Temperature)	2200°F (1204°C)		2400°F (1315°C)		2642°F (1450°C)
Proportional Limit Stress, MPa	170	170	160	150	120
Ultimate Tensile Strength, MPa	320	380	380	260	280
Creep Strain, 103 MPa, 500 hr, air,	~0.4%	~0.4%	~0.4%	0.2%	
Creep Strain, 69 MPa, 500 hr, air,		0.15%	0.15%	0.12%	~0.3%
Rupture Life, 103 MPa, air	~500 hrs	~500 hrs	~500 hrs	>1000 hrs	
Rupture Life, 69 MPa, air					>300 hrs

* Mechanical properties measured in-plane in the 0° direction with a directional fiber content of 18 vol.%.

As discussed earlier, this effect can in large part be attributed to the protective nature of the in-situ grown BN layer on this fiber type since the as-produced strength of the Sylramic-iBN fiber is lower than its precursor Sylramic fiber [**6**], which was used in the N22 panel. However, at the higher CVI SiC matrix content of the N24-C and N26-A systems, there was enough excess silicon in the CVI product to cause fiber attack and UTS degradation even for the Sylramic-iBN fiber. Finally, regarding CMC ultimate strain, the systems with the highest UTS and greatest degree of outside debonding displayed the highest values. The debonding effect can be related to a lower interfacial shear strength (also listed in Table 4), which allowed greater crack openings and greater strain to develop in the CMC. For a given UTS, outside debonding can increase failure strain by as much as 0.2% over inside debonding.

As indicated in Table 1, a key property need for any SiC fiber-reinforced CMC system is the ability to retain to as high a degree as possible its as-fabricated properties under intermediate and high temperature service conditions. At intermediate temperatures, the key issues are oxygen and moisture attack of the interphase coating that can occur on surface-exposed 90° tows even under zero stress, or within the CMC by environmental ingress along random matrix cracks that are being held open by applied CMC loads. To evaluate the CMC systems against the first interphase issue, tensile test specimens from the various panels were exposed to combustion gases in a low-pressure burner rig with the gauge length held at a constant temperature near 800°C (1472°F) for ~100 hours **[7]**. Stress-strain curves at room temperature for three CMC systems after the burner rig exposure are shown in Fig. 10. Significant degradation in UTS was seen for the N22 systems with the Sylramic and Hi-Nicalon Type-S fibers; while excellent UTS retention was seen for the Sylramic-iBN N24-B system. As described earlier, this degradation can be attributed to the removal

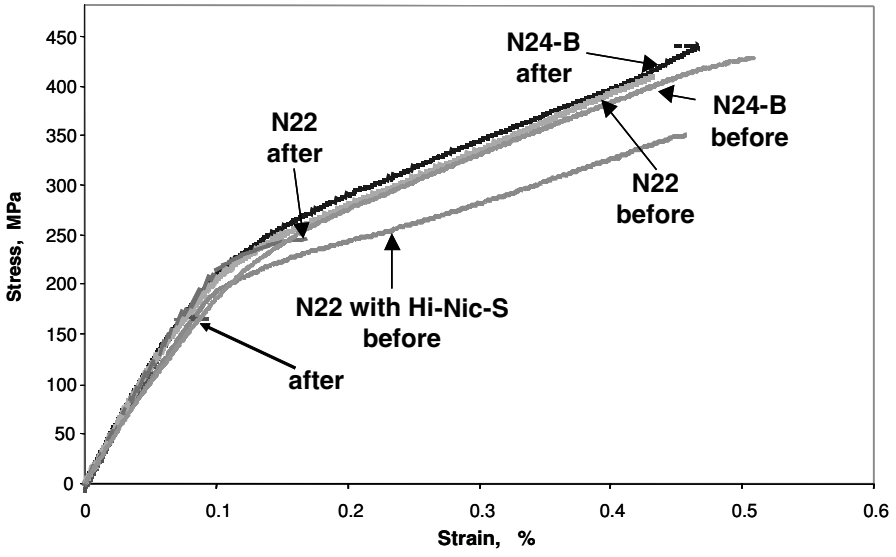

FIGURE 10. Typical room-temperature stress-strain curves for the N22 CMC system with Sylramic and Hi-Nicalon Type-S fibers, and for the N24-B CMC system with Sylramic-iBN fibers before and after combustion gas exposure of the systems in a low-pressure burner rig at ~800°C for ~100 hours. The fibers in the N22 systems each had carbon on their surfaces before BN interphase deposition.

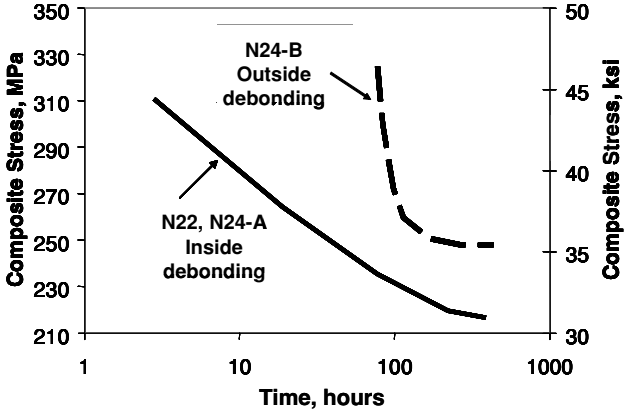

FIGURE 11. Best-fit stress-rupture curves in air at 1500°F (815°C) comparing the inside-debonding N22 and N24-A CMC systems and the outside-debonding N24-B CMC system (total fiber content ∼40 vol.%).

of free carbon on the Sylramic fiber surface (char from Sizing A) and on the as-produced Hi-Nicalon Type-S surface, and to the subsequent silica bonding of contacting fibers. The fact that Fig. 10 shows no loss in UTS for the Sylramic-iBN CMC can be attributed in part to the in-situ BN layer, which minimizes direct contact between SiC fibers, but primarily to the non-detection of detrimental carbon at the interface between the fiber and BN. Thus inadvertent free carbon on fiber surfaces must be avoided for CMC components within combustion environments.

To evaluate the CMC systems against the second interphase issue, tensile test specimens from the various CMC panels were subjected to stress-rupture testing in ambient air at 1500°F (815°C) at stresses above matrix cracking. Final CMC rupture typically occurred when sufficient silica bonding existed between crack-bridging fibers so that when one fiber ruptured due to time-dependent slow crack growth, it caused fracture of its neighbors and the CMC **[20]**. Fig. 11 compares the rupture behavior for the inside debonding systems N22 and N24-A against the first outside debonding system N24-B. Clearly the outside debonding system shows enhanced behavior in that the CMC life is longer for a given applied stress or that a higher stress can be applied to the CMC for a given CMC rupture life. As suggested by Fig. 3 and discussed in the N24-B processing section, this enhanced behavior is due to the Si-doped BN interphase remaining on the Sylramic-iBN fiber surface after matrix cracking, thereby providing additional environmental protection. As shown by Fig. 11, this extra protection enhances CMC life at short times by one or two orders of magnitude, but then eventually loses its ability at longer times. Thus if unpredictable matrix cracking should occur at intermediate and high temperatures, the NASA-developed outside debonding systems will increase CMC life and reliability.

The most important goal for each NASA-developed CMC system was to be able to operate under potential component stress levels for long time at its selected upper use temperature (UUT). To evaluate this capability, tensile test specimens from the various CMC panels were subject to creep-rupture testing in ambient air at their goal UUT and at stresses of ∼60% of their room-temperature cracking stress. The primary performance objective was to demonstrate greater than 500-hour life without specimen rupture. Since high-temperature rupture of an initially uncracked CMC is typically controlled by CMC

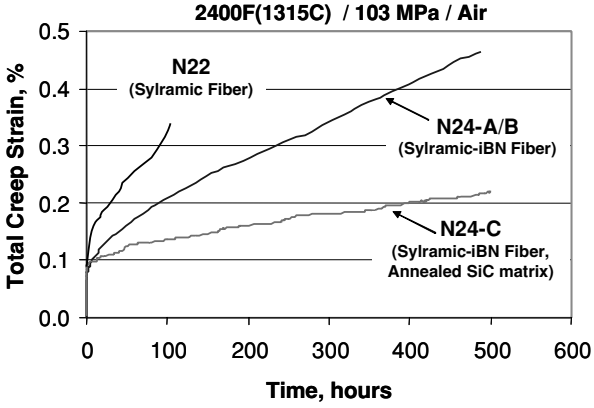

FIGURE 12. Typical total creep strain versus time behavior at 2400°F (1315°C) in air at an applied stress of 103 MPa for the N22 and the N24 CMC systems.

intrinsic creep behavior, another good performance indicator is the ability of a CMC system to display high creep resistance at its UUT and to maintain its creep strain well below a characteristic rupture strain within the 500-hour life goal [**21**]. For example, for test times near 500 hour, the NASA CMC systems typically display a creep-rupture strain of ∼0.4% between 2200 and 2600°F, so that staying at or below this strain level after 500-hour testing should demonstrate the desired performance. Thus, as indicated in Table 4, the N22 system with the Sylramic fiber was able to reach this strain level within 500 hours for an applied stress of 103 MPa at its UUT of 2200°F. However, Fig. 12 shows that under the same stress at 2400°F, the N22 system had a life of only 100 hours, whereas the N24-A system with the Sylramic-iBN fiber had a projected life of greater than 500 hours based on its steady state creep rate. Fig. 12 also shows how annealing of the CVI SiC matrix provided the N24-C system with a projected rupture life of over 1000 hours at 2400°F. However, due to the silicon melt infiltration step for all the N24 CMC systems, these time and temperature condition appear to be the upper limit use conditions based on displaying intrinsic thermal stability under zero stress **[12]**. Finally, Fig. 13 shows the difference in creep-rupture

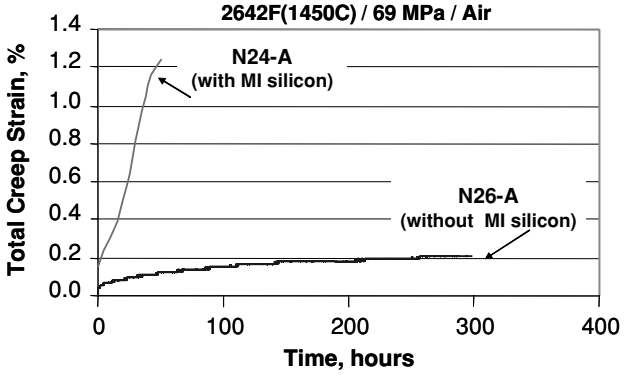

FIGURE 13. Typical total creep strain versus time behavior at 2642°F (1450°C) in air at an applied stress of 69 MPa for the N24-A and N26-A CMC systems.

behavior for a 69 MPa stress at 2642°F between the silicon-containing N24-A system and the silicon-free N26-A system which displayed over 300 hour life capability under these conditions.

5. SUMMARY AND CONCLUSIONS

By working closely with CMC vendors, NASA has been able to identify advanced constituent materials and processes that have yielded various SiC fiber-reinforced SiC matrix composite systems for high temperature structural applications in general and for hot-section engine components in particular. Based on a performance goal of a 500-hour service in air at a stress level of ∼60% that for matrix cracking, these systems have demonstrated upper use temperatures of 2200°F (1204°C), 2400°F (1315°F), and 2600°F (1427°C), which are well above the current capability of the best metallic alloys. This progression in temperature capability is related first to the development of the Sylramic-iBN SiC fiber, then to the development of an annealing step for an improved CVI SiC matrix in the baseline NASA processing route, and finally to the elimination of the silicon melt infiltration step for filling pores in the SiC matrix. Advances in CMC environmental durability were also made at NASA by use of in-situ grown BN fiber surface layers, CVI-deposited Si-doped BN interphase coatings, carbon-free interfaces between the fiber and BN, and processing approaches that cause the CVI BN interphase to remain on the fiber and "outside" debond from the matrix during CMC cracking, thereby allowing the interphase coating to provide extra environmental protection to the crack-bridging fibers.

Although the processing information and property results presented here are limited, they should be sufficient for component designers to select the CMC systems and processes that best meet their component performance requirements, and then to initiate more extensive efforts for system scale-up and component evaluation with a variety of commercial CMC vendors. Although not yet demonstrated, it might be expected that as long as environmental effects do not control the performance of these systems, a time-temperature relationship should exist between projected component service life and CMC system upper use temperature capability. For example, based on typical atomic diffusion in SiC materials, rupture life for each CMC system should change by one order of magnitude for every ∼180°F (100°C) difference between the component's upper service temperature and the system's upper use temperature capability **[12]**. Thus the 2600°F system should be able to perform for ∼5000 hours at 2420°F, but only ∼50 hours at 2780°F. Stress effects will also have an influence CMC component life, but these should be evaluated for sub-elements of the components on a case-by-case basis.

6. ACKNOWLEDGEMENTS

The authors gratefully acknowledge (1) the funding support of the NASA Enabling Propulsion Materials (EPM) program, the NASA Ultra Efficient Engine Technology (UEET) program, and the NASA Glenn Director's Discretionary Fund; (2) the professional support of L. Thomas-Ogbuji and J. Hurst; and (3) the technical support of R. Phillips, R. Babuder, and R. Angus.

7. REFERENCES

1. D. Brewer, HSR/EPM Combustor Materials Development Program, *Materials Science and Engineering*, **A261**, 284–291 (1999).
2. NASA Ultra Efficient Engine Technology (UEET) Program, http://www.grc.nasa.gov/WWW/RT2000/2000/2100shaw.html
3. NASA Next Generation Launch Technology (NGLT) Program, http://www1.msfc.nasa.gov/NEWSROOM/background/facts/ngltfacts.pdf
4. K.N. Lee, D.S. Fox, R.C. Robinson, and N.P. Bansal, Environmental Barrier Coatings for Silicon-Based Ceramics, in *High Temperature Ceramic Matrix Composites*, W. Krenkel, R. Naslain, and H. Schneider, Eds, Wiley-VCH, Weinheim, Germany, (2001), pp. 224–229.
5. J.L. Smialek, R.C. Robinson, E.J. Opila, D.S. Fox, and N.S. Jacobson, SiC and Si_3N_4 Recession Due to SiO_2 Scale Volatility under Combustor Conditions, *Adv. Composite Mater*, **8** [1], 33–45 (1999).
6. J.A. DiCarlo and H-M. Yun, Non-Oxide (Silicon Carbide) Ceramic Fibers, in *Handbook of Ceramic Composites,* N.P. Bansal, Ed., Kluwer Academic Publishers, Boston, MA, 2004, pp. 33–52.
7. L. Thomas-Ogbuji, A Pervasive Mode of Oxidation Degradation in a SiC/SiC Composite, *J. Am. Ceram. Soc*., **81** [11], 2777–2784 (1998).
8. H-M. Yun, and J.A. DiCarlo, Comparison of the Tensile, Creep, and Rupture Strength Properties of Stoichiometric SiC Fibers, *Cer. Eng. Sci. Proc*., **20** [3], 259–272 (1999).
9. G.N. Morscher, H-M. Yun, J.A. DiCarlo, and L. Thomas-Ogbuji, Effect of a BN Interphase that Debonds Between the Interphase and the Matrix in SiC/SiC Composites, *J. Am. Ceram. Soc.*, **87**, 104–112 (2004).
10. R.T. Bhatt, NASA Glenn *Research and Technology* 2003, NASA/TM—2004–212729, 20–21 (2004).
11. R.T. Bhatt, T.R. McCue, and J.A. DiCarlo, Thermal Stability of Melt Infiltrated SiC/SiC Composites, *Cer. Eng. Sci. Proc*., **24** [4B], (2003), 295–300.
12. J.A. DiCarlo, R.T. Bhatt, and T.R. McCue, Modeling the Thermostructural Stability of Melt Infiltrated SiC/SiC Composites, *Cer. Eng. Sci. Proc.,* **24** [4B], (2003), 465–470.
13. Starfire Systems, http://www.starfiresystems.com/
14. G.S. Corman and K.L. Luthra, Silicon Melt Infiltrated Ceramic Composites (HiPerComp^{TM}), in *Handbook of Ceramic Composites*, N.P. Bansal, Ed., Kluwer Academic Publishers, Boston, MA, 2004, pp. 99–115.
15. S.K. Mital, P.L.N. Murthy, and J.A. DiCarlo, Characterizing the Properties of a Woven SiC/SiC Composite, *Journal of Advanced Materials*, **35** [1], 52–60 (2003).
16. Z. Li and R.C. Bradt, Thermal Expansion of the Cubic (3C) Polytype of SiC, *J. Mater. Sci*. **21** (1986), 4366–68.
17. J.A. DiCarlo, Creep of Chemically Vapour Deposited SiC Fibers, *J. Mater. Sci*. **21** (1986), 217–224.
18. *Thermophysical Properties of Matter, Thermal Conductivity, Nonmetallic Solids*, Vol. 2, Y.S. Touloukia el al., Eds., Plenum, New York, (1970), p. 6a.
19. G.N. Morscher, Stress-Dependent Matrix Cracking in 2D Woven SiC-fiber Reinforced Melt-Infiltrated SiC Matrix Composites, *Comp. Sci. Tech.*, in print.
20. G.N. Morscher and J.D. Cawley, Intermediate Temperature Strength Degradation in SiC/SiC Composites, *J. European Ceram. Soc.*, **22**, 2777–2787 (2002).
21. J.A. DiCarlo, H.M. Yun, and J.B. Hurst, Fracture Mechanisms for SiC Fibers and SiC/SiC Composites Under Stress-Rupture Conditions at High Temperatures, *Applied Mathematics and Computation*, **152**, 473–481(2004).